Journal of Advanced Research 73 (2025) 397–410

Contents lists available at ScienceDirect

Journal of Advanced Research

journal homepage: www.elsevier.com/locate/jare

Original Manuscript

Dual-species proteomics and targeted intervention of animal-pathogen interactions

Yang Sylvia Liu [a,1], Chengqian Zhang [b,1], Bee Luan Khoo [c,d,e], Piliang Hao [b,*], Song Lin Chua [a,f,g,**]

[a] Department of Applied Biology and Chemical Technology, The Hong Kong Polytechnic University, Kowloon, Hong Kong Special Administrative Region
[b] School of Life Science and Technology, ShanghaiTech University, China
[c] Department of Biomedical Engineering, City University of Hong Kong, Hong Kong Special Administrative Region
[d] Hong Kong Center for Cerebro-Cardiovascular Health Engineering (COCHE), Hong Kong Special Administrative Region
[e] City University of Hong Kong-Shenzhen Futian Research Institute, Shenzhen, China
[f] State Key Laboratory of Chemical Biology and Drug Discovery, The Hong Kong Polytechnic University, Kowloon, Hong Kong Special Administrative Region
[g] Research Centre for Deep Space Explorations (RCDSE), The Hong Kong Polytechnic University, Kowloon, Hong Kong Special Administrative Region

HIGHLIGHTS

- Dual-species SILAC proteomic method showed host and microbe proteomes simultaneously.
- *Pseudomonas aeruginosa* upregulated PvdA and pyoverdine in *Caenorhabditis elegans* intestine.
- *C. elegans* correspondingly upregulated ferritin (Ftn-2) in response to pyoverdine.
- Galangin inhibited pyoverdine production and biofilm formation.
- Galangin-ciprofloxacin combinatorial therapy eliminated wound infection in Medaka fish.

GRAPHICAL ABSTRACT

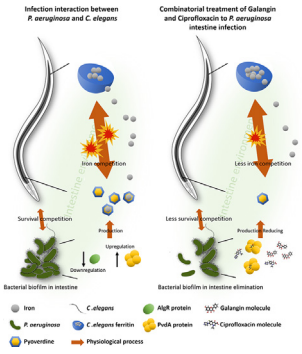

ARTICLE INFO

Article history:
Received 15 June 2024
Revised 30 August 2024
Accepted 31 August 2024
Available online 2 September 2024

Keywords:
SILAC proteomics
Pseudomonas aeruginosa
Caenorhabditis elegans
Host-microbe interactions
Iron competition

ABSTRACT

Introduction: Host-microbe interactions are important to human health and ecosystems globally, so elucidating the complex host-microbe interactions and associated protein expressions drives the need to develop sensitive and accurate biochemical techniques. Current proteomics techniques reveal information from the point of view of either the host or microbe, but do not provide data on the corresponding partner. Moreover, it remains challenging to simultaneously study host-microbe proteomes that reflect the direct competition between host and microbe. This raises the need to develop a dual-species proteomics method for host-microbe interactions.

Objectives: We aim to establish a forward + reverse Stable Isotope Labeling with Amino acids in Cell culture (SILAC) proteomics approach to simultaneously label and quantify newly-expressed proteins of host and microbe without physical isolation, for investigating mechanisms in direct host-microbe interactions.

Methods: Using *Caenorhabditis elegans-Pseudomonas aeruginosa* infection model as proof-of-concept, we employed SILAC proteomics and molecular pathway analysis to characterize the differentially-expressed microbial and host proteins. We then used molecular docking and chemical characterization to identify chemical inhibitors that intercept host-microbe interactions and eliminate microbial infection.

* Corresponding author.
** Corresponding author at: Department of Applied Biology and Chemical Technology, The Hong Kong Polytechnic University, Kowloon, Hong Kong Special Administrative Region.
E-mail addresses: haopl@shanghaitech.edu.cn (P. Hao), song-lin.chua@polyu.edu.hk (S.L. Chua).
[1] These authors contributed equally to this work.

https://doi.org/10.1016/j.jare.2024.08.038

Results: Based on our proteomics results, we studied the iron competition between pathogen iron scavenger and host iron uptake protein, where *P. aeruginosa* upregulated pyoverdine synthesis protein (PvdA) (fold-change of 5.2313) and secreted pyoverdine, and *C. elegans* expressed ferritin (FTN-2) (fold-change of 3.4057). Targeted intervention of iron competition was achieved using Galangin, a ginger-derived phytochemical that inhibited pyoverdine production and biofilm formation in *P. aeruginosa*. The Galangin-ciprofloxacin combinatorial therapy could eliminate *P. aeruginosa* biofilms in a fish wound infection model, and enabled animal survival.

Conclusion: Our work provides a novel SILAC-based proteomics method that can simultaneously evaluate host and microbe proteomes, with future applications in higher host organisms and other microbial species. It also provides insights into the mechanisms dictating host-microbe interactions, offering novel strategies for anti-infective therapy.

Introduction

Host-microbe interactions are integral to global ecosystems and in humans, so understanding these relationships is important to address global challenges in infectious diseases and climate change. Systems biology approaches are increasingly employed to study host-microbe interactions, because of the technical advances in specificity and sensitivity. Quantitative proteomics are used widely to study either microbe or host proteomics in an infection [1,2], but it is important to note that proteomics was typically performed only on the host after treatment with microbial proteins or microbe itself (from the point of view of the host) [3,4], or on the microbe after interactions with the host (from the point of view of microbe) [5,6]. This implied that researchers can only acquire one-sided proteomic data from either the host or microbe, without gaining proteomic perspectives from the other partner. In an effort to elucidate novel host-microbe interactions, host and microbe co-study using proteomics is gaining traction in recent years [7,8]. Ideally, dual-species proteomics quantifies proteins of microbes and animal host in a single experiment, and provides insights into both host and microbial responses during interactions. However, many strategies require pre-isolation steps which are destructive and difficult to study small bacterial populations in the larger host [5].

One accurate and sensitive proteomics technique frequently used to label eukaryotic proteomes for liquid chromatography-mass spectrometry (LC-MS) analysis is Stable Isotope Labeling with Amino acids in Cell culture (SILAC) [9–11]. However, its application in studying both animal and microbe is limited, due to difficulty in labeling both entire animal and microbes and only entire single-celled organisms or embryos can be labelled completely alive [12,13]. This provides a rationale for us to develop a SILAC-based proteomics approach to simultaneously characterize host and microbial physiologies during their interactions, especially infections.

Bacterial pathogens establish chronic infections by forming biofilms on host tissues and medical implants [14], where 80 % bacterial infections attributed to biofilms [15]. Biofilms are bacterial aggregates embedded in protective exopolymeric substances (EPS) [16], allowing bacteria to attain extreme resistance to antimicrobials and host clearance [17,18]. As model organism for biofilm research and member of the dangerous ESKAPE pathogens [19], *Pseudomonas aeruginosa* is a Gram negative pathogen that causes infections in hospitalized patients, immunocompromised individuals and elderly, where mortality rate for bacteremia can reach 39 % [20,21]. *P. aeruginosa* could infect the respiratory system [22], and the intestinal tract, such as gut-derived sepsis, Shanghai fever and severe necrotizing enterocolitis [23–26]. The intestinal tract is also an important reservoir for *P. aeruginosa* opportunistic infections and dissemination to the lungs [27]. Moreover, *P. aeruginosa* infections could range from localized infections of the skin to life-threatening systemic diseases or seed following bloodstream infections [28,29].

P. aeruginosa employs a plethora of virulence factors for establishing biofilm-mediated infections. Its ability to produce the sticky biofilm matrix, which comprises of exopolysaccharides, adhesion proteins and extracellular DNA (eDNA), to prevent antibiotics and immune cells from accessing the biofilm cells [30]. Another virulence factor is pyoverdine, which is a secreted self-fluorescent siderophore important for uptake of iron from the environment and biofilm formation [31]. Biofilm formation and pyoverdine production are mainly attributed to c-di-GMP secondary messenger signaling, which is ubiquitous in many bacterial species [32,33].

To study P. aeruginosa virulence of intestine infection, Caenorhabditis elegans is commonly used as an experimental host for establishing simple intestinal infection model [34,35]. This is because *C. elegans* possesses similar mechanisms of immune defense with orthologs in mammals and invertebrates [36]. Due to these universal host responses, microbial pathogenesis has evolved correspondingly, where bacterial pathogens share similar host-infection strategies. For instance, *C. elegans* upregulated immune response genes, such as autophagy pathway and lysozymes, while different pathogens upregulated host invasion proteins [37–40]. Development of anti-virulence agents that interfere host-pathogen interactions will tilt the balance in favor of the host [41], leading to the elimination of pathogens and recovery from infectious diseases.

Iron is a vital nutrient for both host and pathogen, but its availability is often limited in the host's extracellular environment due to sequestration mechanisms. As a result, host-pathogen interactions are often characterized by intense competition for this essential nutrient [42–44]. In response to this competition, both hosts and pathogens have evolved various strategies to acquire iron. For instance, pathogens secrete iron-chelating siderophores such as staphyloferrin in Staphyloccoccus aureus [45], while hosts produce iron uptake proteins such as lactoferrin. The identification of strategies used by both host and pathogen to compete for iron has led to the development of novel anti-virulence therapies that target these pathways, potentially reducing pathogen virulence and improving host outcomes.

Here, we aim to develop a novel dual-species proteomics method to study host-microbe interactions, with the specific objectives of elucidating pathogenesis mechanisms and developing novel anti-infective therapy. Using a *C. elegans* host-*P. aeruginosa* pathogen interaction model as proof-of-concept, we established a concurrent forward (host)-reverse (microbe) SILAC proteomics approach to label and quantify newly synthesized host and pathogen proteins after *P. aeruginosa* establish infections in the *C. elegans* intestine. The rationale for using this model was because it is simple model which can be easily tagged and observed for studies, and we had previously established this model for infection studies [34,46–48]. For the host, its ^{12}C light lysine-proteins will

incorporate ^{13}C heavy lysine in its newly synthesized proteins, while the^{13}C heavy lysine-labeled pathogen will correspondingly incorporate ^{12}C- $_{L}$-lysine into its proteins during host infection. This represents a technical advance over existing proteomics techniques that only evaluate either host or microbe proteomes.

To validate our proteomics data, we chose to evaluate the iron competition between the host and microbe, where *P. aeruginosa* upregulated its expression of pyoverdine synthesis proteins (PvdA), whereas *C. elegans* expressed the ferritin protein (FTN-2). Pyoverdine is a secreted siderophore important for scavenging iron from the environment and biofilm formation [31]. Although a previous study had shown that FTN-2 was part of the immune network upregulated in response to *S. aureus* [49], we showed for the first time that pyoverdine was the direct iron competitor of FTN-2, which addressed the knowledge gap on the interacting partner of FTN-2.

To interfere effective iron competition by the pathogen, we employed structure-based virtual screening to identify Galangin (3,5,7-trihydroxyflavone), a ginger-derived phytochemical which can potentially bind to and inhibit the PvdA active site. Galangin could reduce expression of *pvdA* gene and production of pyoverdine at 22.69 μM. As we showed that Galangin could inhibit biofilm formation via pyoverdine inhibition, a proof-of-concept Galangin-ciprofloxacin combinatorial therapy could effectively eliminate *P. aeruginosa* infection and promote host survival.

Hence, our study is unique in developing the dual-species SILAC proteomics approach that can provide on proteins expressed in both host and microbe, which serves as a significant advance over our prior SILAC proteomics research that study the effects of antibiotics on bacterial biofilms [50]. Next, the data generated from our proteomics method can be used to study host-microbe interactions and develop novel anti-infective therapeutics, with potential to eliminate *P. aeruginosa* infections. This adds on to our existing work on iron competition between host and microbe [51,52], and contributes to more therapeutic options against *P. aeruginosa* infections [53,54].

Using forward-reverse SILAC to study animal-bacterial interactions

As proof-of-concept, we employed a *C. elegans-P. aeruginosa* infection model by feeding the nematodes with *P. aeruginosa* biofilms. We had previously shown that *P. aeruginosa* formed biofilms on the agar [46,55]. We monitored the feeding of *P. aeruginosa* into *C. elegans* intestines after 6 h post infection (h.p.i) (early feeding) and 24 h.p.i. (late feeding), where there was increase in viable bacterial counts (Fig. 1**A**) and live *gfp*-tagged bacteria within the intestine (Fig. 1**B).** This indicated that *P. aeruginosa* colonized and remained viable in the *C. elegans* intestine, while its GFP production indicated that they were metabolically active.

To understand the overall interactions between *C. elegans* and intestinal *P. aeruginosa*, we modified and established a forward-reverse SILAC workflow (Fig. 1**C**), which could study new protein abundances in the intestinal *P. aeruginosa* and animal host quickly and accurately by labeling host and bacterial proteins simultaneously without the need for physical isolation. The SILAC proteomic approach is commonly used to determine changes in protein expression induced by experimental conditions in mammalian cell culture [56,57], with few applications in prokaryotes [50,58,59]. Our SILAC approach broadened the scope of SILAC proteomics, where mechanisms of host-pathogen interactions could be identified and applied to other bacterial species.

To ensure that *P. aeruginosa* could only incorporate $_{L}$-lysine for SILAC labelling, we employed the *P. aeruginosa* mutant that cannot self-synthesize lysine, mPAO1Δ*lysA* and requires exogenous lysine to survive [50]. We previously showed that the Δ*lysA* mutant with $_{L}$-lysine supplements had similar growth rates and metabolism as wild-type PAO1 [50]. Within the context of this study, we also showed that as long as the medium was supplemented with $_{L}$-lysine, the Δ*lysA* mutant could colonize and infect *C. elegans* intestine, and kill the animal over time in a similar fashion as wild-type PAO1 (Supplementary Figure 1). As for *C. elegans*, lysine is a dietary essential amino acid [60], with 93 % incorporation of labelled lysine into its proteins [61], so the animal could be directly used for our proteomic approach.

Hence, the Δ*lysA* mutant prelabeled with 'heavier' ^{13}C- $_{L}$-lysine were initially fed to *C. elegans* whose proteins contain 'lighter' ^{12}C- $_{L}$-lysine. Over the course of host-microbial interactions, intestinal *P. aeruginosa* could incorporate ^{12}C- $_{L}$-lysine from the host in its newly synthesized proteins, while *C. elegans* would instead incorporate ^{13}C- $_{L}$-lysine e from intestinal *P. aeruginosa* in its new proteins. The Q-Exactive HF-X Hybrid Quadrupole-Orbirap Mass spectrometer system was employed to analyze the SILAC samples, where we identified more than 4000 proteins differentially expressed by *C. elegans* and *P. aeruginosa* from established databases (WormBase for *C. elegans* [62] and Pseudomonas.com for *P. aeruginosa* [63]) using the Proteome Discoverer software (PD) [64]. Only proteins that were differentially expressed at higher (>2-fold) or lower (<0.5-fold) levels in triplicate samples at 24 h.p.i than 6 h.p.i were shortlisted for further analysis.

We hypothesized that the actively expressed proteins by the host and pathogen are important in conferring competitive advantages over the other. A total of 752 proteins from *P. aeruginosa* and 3386 proteins from *C. elegans* were subjected to MetaboAnalyst 5.0 for statistical analysis [65]. For the multivariate analysis of *P. aeruginosa* and *C. elegans* proteins, the principal component analysis (PCA) plot (Fig. 2**A-B**) revealed that the 6 h.p.i group and 24 h.p.i group were clustered separately. The PCA plot of *P. aeruginosa* was performed with the 61.9 % of total variance between these two groups represented by the first two principal components (Fig. 2**A**). The principal component 1 (PC1) and principal component 2 (PC2) explained 43 % and 18.9 % of the variance (Fig. 2**A**). For multivariate analysis of *C. elegans* proteins, the principal component analysis (PCA) plot revealed that two groups were with the 85 % of total variance represented by the first two principal components (Fig. 2**B**). The principal component 1 (PC1) and principal component 2 (PC2) explained 72.7 % and 12.3 % of the variance (Fig. 2**B**). The volcano plot combines a measure of statistical significance from statistical analysis with the magnitude changes [66]. These dots (blue: downregulated, red: upregulated) in volcano plot of *P. aeruginosa* (Fig. 2**C**) and *C. elegans* (Fig. 2**D**) indicates different proteins that display both large magnitude fold-changes (x axis) and high statistical significance (−log10 of p values, y axis).

Protein AlgR (gene = *algR*) and PvdA (gene = *pvdA*) of *P. aeruginosa* were downregulated and upregulated with a log2 (FC) value of −6.7367 (pvalue = 0.0018066) and 5.2313 (pvalue = 0.033246) respectively (Fig. 2**C**). Protein FTN-2 of C. elegans was upregulated with a log2 (FC) value of 3.4057 (pvalue = 0.0016067) (Fig. 2**D**). According to the standards of Functional Classifications Manually Assigned by PseudoCAP for bacteria[67], the upregulated and downregulated proteins of *P. aeruginosa* were classified into different functional groups (Fig. 2**E** and Supplementary figure 2).

Our initial analysis revealed that for *P. aeruginosa*, a large proportion (14 %) of motility and attachment proteins were upregulated from 6 h.p.i to 24 h.p.i (Fig. 2**E**), which corroborated with previous findings that motility and surface attachment are important in bacterial colonization in the host [68]. After uploading proteins information of *C. elegans* to KEGG database, the pathway enrichment of proteins set was analyzed through clusterProfiler package in R. From the gene ratio in the dot plot (Fig. 2**F**), the most enriched KEGG pathways were carbon metabolism, ribosome and oxidative phosphorylation, which were similar to previous study

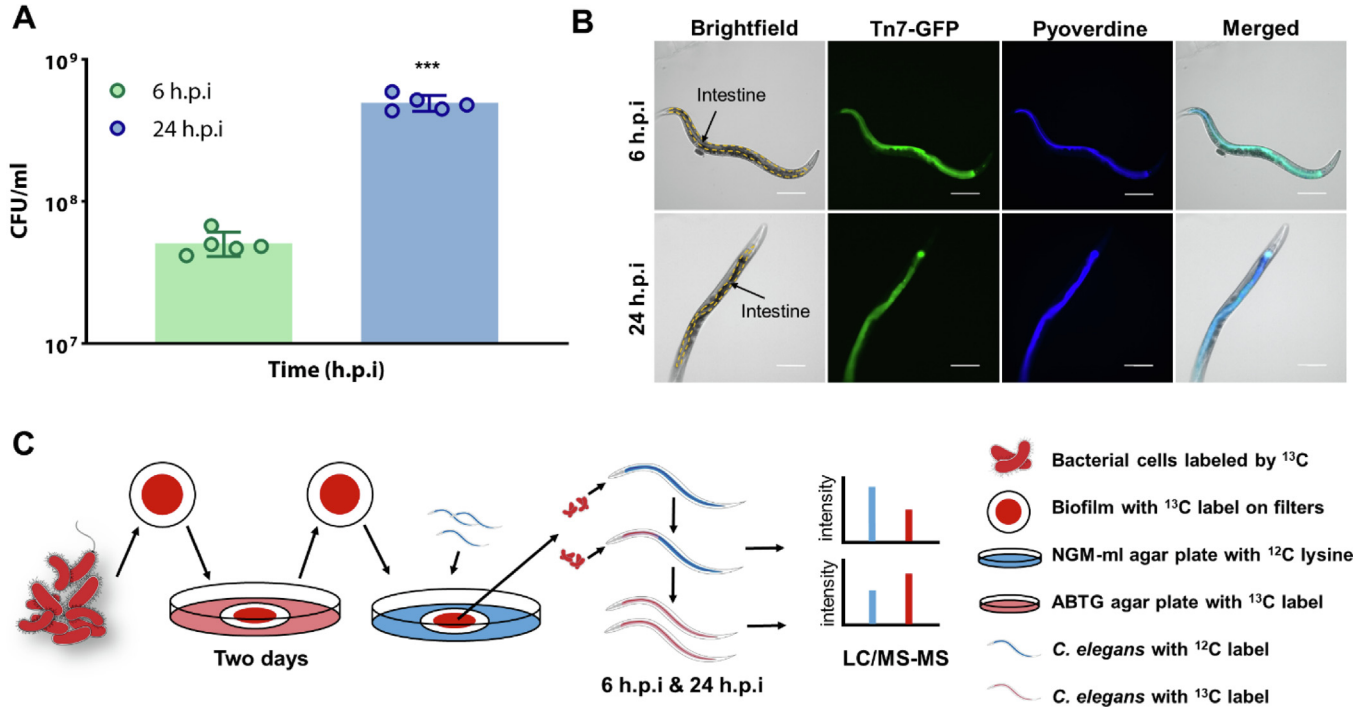

Fig. 1. Workflow of SILAC proteome analysis of *Caenorhabditis elegans-Pseudomonas aeruginosa* host-pathogen interaction model. (**A**) *P. aeruginosa* population numbers in intestine at 6 h.p.i and 24 h.p.i. (**B**) Fixed *C. elegans* with *gfp*-tagged PAO1 in intestine at 6 h.p.i and 24 h.p.i. (**C**) The workflow and experimental design of this project, including the *P. aeruginosa* – *C. elegans* infection model and the SILAC proteomics assay. Δ*lysA* mutant labeled with ^{13}C- $_{L}$-lysine was cultivated on agars which contained ^{13}C- $_{L}$-lysine for two days to form biofilm. The samples were then collected for the SILAC proteomics assay. H.p.i = hours post-infection. Scale bar: 100 μm. ***P < 0.001.

[69]. According to the WormBase gene ontology for *C. elegans*, upregulated and downregulated proteins from host were functionally grouped in Supplementary figure 3 respectively. This indicated that our SILAC approach was reliable in detecting changes in protein expression accurately.

Interestingly, among bacterial proteins, we observed that the positive alginate biosynthesis regulatory protein AlgR [70] was significantly downregulated, while L-ornithine N(5)-monooxygenase PvdA [71] was upregulated from 6 h.p.i to 24 h.p.i. AlgR is a regulator involved in the expression of multiple virulence factors, such as pyoverdine and other iron acquisition genes (PvdS) [72,73], whereas PvdA is involved in the biosynthesis of pyoverdine, an iron siderophore important for microbial growth [74]. Correspondingly, *C. elegans* upregulated the expression of FTN-2 (ferritin), an iron scavenging protein commonly found in most eukaryotes [75]. Since both host and pathogen upregulated their mechanisms important in iron uptake, this raised the rationale that the pathogen and animal used pyoverdine and ferritin respectively to compete for iron. While pyoverdine was recently implicated in *C. elegans* intestinal infection [76] and ferritin was involved in innate immune response [49], it was unclear if both were direct iron competitors in *C. elegans* infection.

Downregulation of algR promotes pyoverdine production in C. elegans

Since our proteomics data revealed a correlative downregulation of AlgR and PvdA upregulation, we next aim to show that intestinal *P. aeruginosa* had lower AlgR expression to increase PvdA expression within *C. elegans* intestine, where pyoverdine was the virulence factor that caused *C. elegans* death. The *pvdA* gene expression [35] and corresponding pyoverdine production was upregulated in intestinal wild-type PAO1 within *C. elegans* from 6 h.p.i to 24 h.p.i, whereas the Δ*pvdA* mutant did not (Fig. 3**A-B**). Hence, we observed that the Δ*pvdA* mutant lost its ability to kill *C. elegans*, which can be restored with the *pvdA* complementation (Fig. 3**C**). The expression of *pvdA* was inversely regulated by *algR* gene. The Δ*algR* mutant displayed higher expression of *pvdA* gene and pyoverdine levels than wild-type PAO1 and Δ*pvdA* (Fig. 3**A-B**), which confirmed the findings from proteomic data. This had severe implications in the animal host, where the Δ*algR* mutant could kill *C. elegans* at a higher and faster rate than wild-type PAO1 (Fig. 3**C**). Gene complementation in Δ*algR* mutant restored inability by *P. aeruginosa* to effectively kill the populations (Fig. 3**C**). This corroborated with previous study that AlgR expression repressed pyoverdine production [77]. Hence, this showed that the downregulation of AlgR resulted in the higher expression of pyoverdine, which was crucial in killing the host animals.

Host ferritin is involved in iron competition with bacterial pyoverdine

From the point of view of *C. elegans* host, our proteomics data revealed the upregulation of FTN-2 protein which was involved in iron metabolism [78]. By using the *ftn-2*(ok404) mutant animal (RB668) deficient in ferritin production, we surprisingly observed that it did not elicit the iron scavenging response from *P. aeruginosa*. In wild-type animals, *P. aeruginosa* upregulated *pvdA* gene expression and pyoverdine production (Fig. 4**A-C**). However, there was subdued *pvdA* expression and lower associated pyoverdine levels by intestinal *P. aeruginosa* when colonizing *ftn-2*(ok404) mutant animal (Fig. 4**A-C**). Interestingly, the *ftn-2*(ok404) mutant animals could survive better than wild-type N2 animals upon *P. aeruginosa* infection (Fig. 4**C**). This indicated that without the host iron competitor (FTN-2), the intestinal bacteria did not seem to activate its pyoverdine operon, thereby negating the iron competition between host and pathogen.

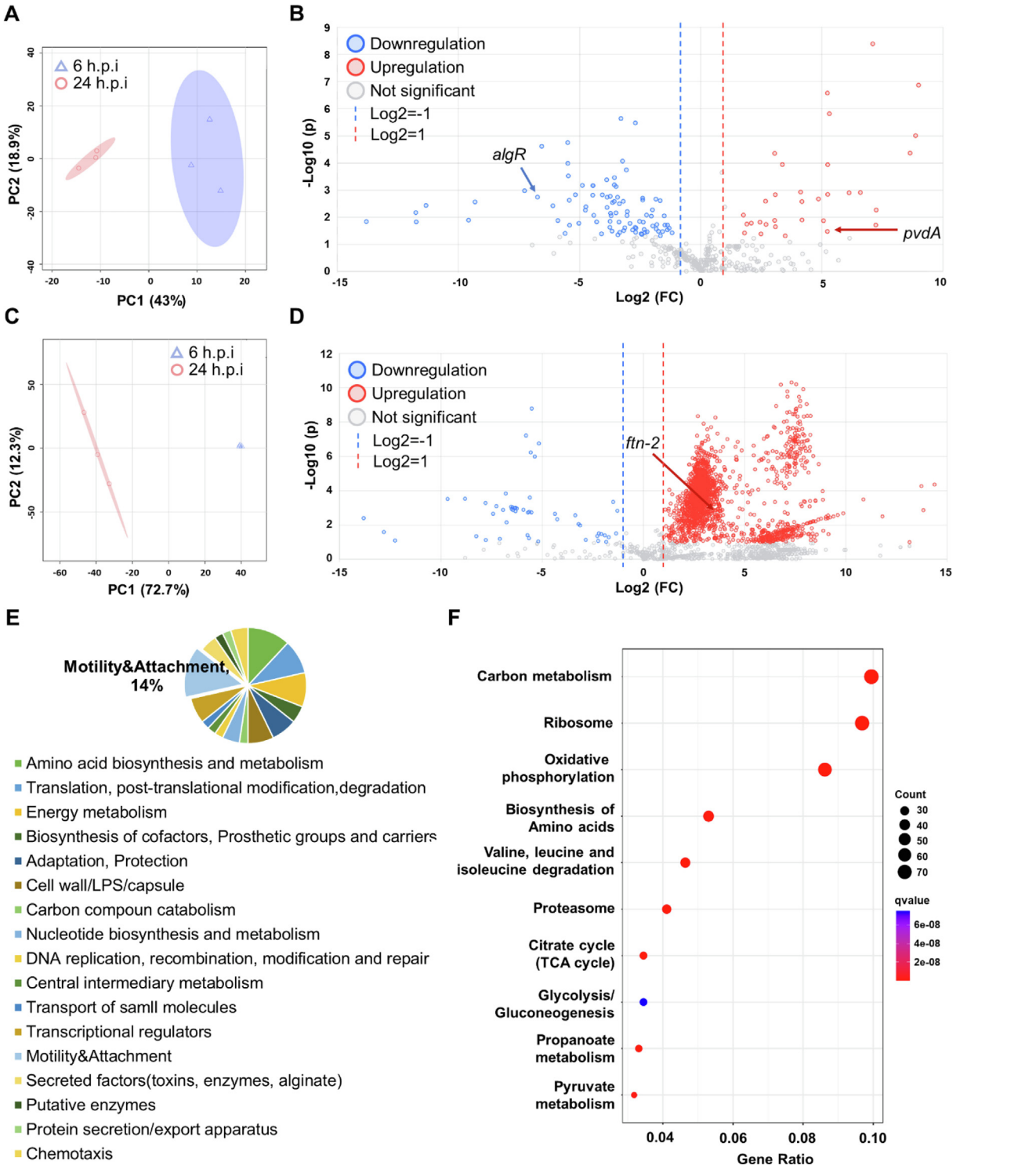

Fig. 2. Proteomic profiling of proteins in *Pseudomonas aeruginosa* and *Caenorhabditis elegans* during interactions. (**A**) The PCA score plots showed that the proteins of *P. aeruginosa* samples from 6 h.p.i and 24 h.p.i groups were clustered separately. (**B**) Volcano plot representation of differential expression analysis of proteins in *P. aeruginosa* samples from 6 h.p.i and 24 h.p.i groups. (**C**) The PCA score plots showed that the proteins of *C. elegans* samples from 6 h.p.i and 24 h.p.i groups were clustered separately. (**D**) Volcano plot representation of differential expression analysis of proteins in *C. elegans* from 6 h.p.i and 24 h.p.i groups. (**E**) Functional groups of upregulated proteins of *P. aeruginosa* from 6 h.p.i to 24 h.p.i. The Motility & Attachment took a large proportion in upregulated groups. (**F**) Significantly enriched KEGG pathways of the upregulated proteins from *C. elegans*.

Galangin is a pyoverdine inhibitor that interferes host-pathogen interactions

To intervene iron competition between host and pathogen and tile the favor towards the host, we next aim to develop an anti-virulence strategy that inhibits PvdA and intercept pyoverdine synthesis in *P. aeruginosa*. While iron chelators such as EDTA and DIPY were previously proposed as anti-pyoverdine strategies [79,80], these chemicals may have pleiotropic effects, thereby requiring inhibitors specific against pyoverdine synthesis proteins.

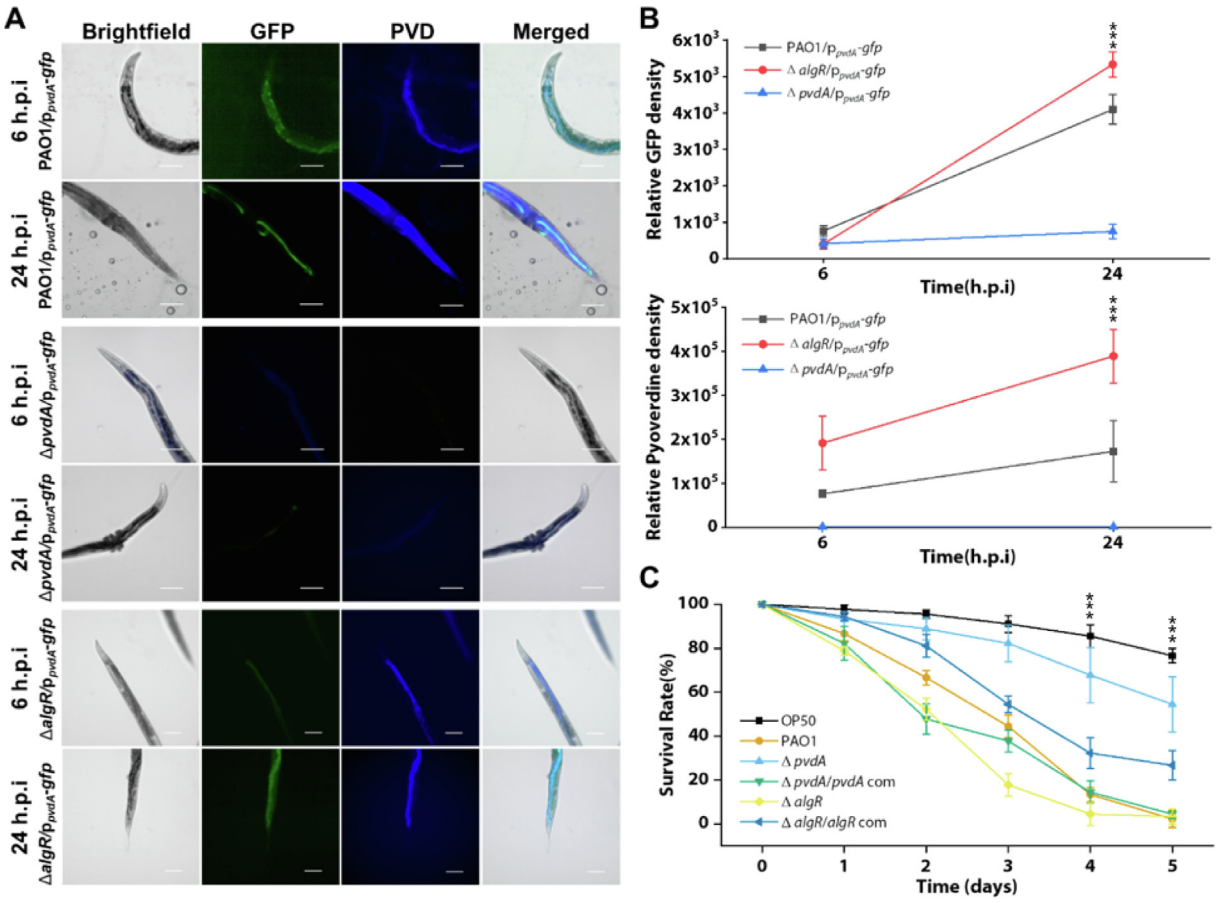

Fig. 3. ***Pseudomonas aeruginosa*** **upregulates pyoverdine expression via repression of AlgR and enhancing of PvdA in intestinal infection of** ***Caenorhabditis elegans.*** (**A**) Representative fluorescent images of the fixed nematode's intestine after the infection of PAO1/p$_{pvdA}$-*gfp*, Δ*pvdA*/p$_{pvdA}$-*gfp* and Δ*algR*/p$_{pvdA}$-*gfp* from 6th to 24th hour. GFP is green, and Pyoverdine channel is blue. Scale bars, 50 μm. (**B**) Relative GFP fluorescence density and pyoverdine density from wild-type (N2) nematodes infected by PAO1/p$_{pvdA}$-*gfp*, Δ*pvdA*/p$_{pvdA}$-*gfp* and Δ*algR*/p$_{pvdA}$-*gfp* from 6th to 24th hour. (**C**) Nematodes were cultivated on different bacterial mutants' lawn for 5 days. The survival rate of nematodes was recorded. H.p.i = hours post-infection. Scale bar: 100 μm. ***P < 0.001.

Another inhibitor (5-fluorocytosine) also targeted PvdS, regulator in the *pvd* synthesis pathway [81].

We employed structure-based virtual screening to identify potential inhibitors from the natural product compounds library that competitively bind to the active site of PvdA protein [82]. We preliminary identified Galangin, a flavonoid which potentially bind to the PvdA's active site in a similar position as the N∼5 ∼ -hydroxy-L-ornithine (ONH) ligand at stronger binding affinity (−6.7 kcal/mol for Galangin as compared to −4.8 kcal/mol for ligand) (Fig. 5**A**). Moreover, Galangin could inhibit *pvdA* gene expression (Fig. 5**B**) and pyoverdine levels (Fig. 5**C**), where the half-maximal inhibitory concentration (IC_{50}) is 22.69 μM (Fig. 5**D**).

Although PvdA inhibition of Galangin is not bactericidal (Supplementary Fig. 4), this might prevent the pathogen from establishing effective infection in the host, so its combinatorial therapy with an antibiotic was expected to enhance the killing of pathogen in disease treatment. As proof-of-concept, we employed ciprofloxacin, which is widely used for the treatment of biofilm infections caused by *P. aeruginosa* [83]. In *in vitro* assays, ciprofloxacin could inhibit *P. aeruginosa* biofilm growth with an IC_{50} of 0.04 μg/ml, and the minimal concentration of Galangin in combination with ciprofloxacin that could inhibit bacterial biofilm growth was 12.5 μM and 0.04 μg/ml respectively from the CFU results (Supplementary figure 5). Since higher doses of antimicrobials are typically expected for *in vivo* animal studies [84], we evaluated the efficacy of 25 μM Galangin-0.08 μg/ml ciprofloxacin combinatorial treatment against the *C. elegans* intestinal infection. Although Galangin and ciprofloxacin monotherapies could reduce pyoverdine levels in *C. elegans* (Fig. 5**E-F**), they had mild killing effect on intestinal *P. aeruginosa* populations (Fig. 5**G**). Instead, the Galangin-ciprofloxacin combinatorial treatment could significantly downregulate pyoverdine levels (Fig. 5**E-F**) and eliminate *P. aeruginosa* in the animal intestine (Fig. 5**G**), resulting in enhanced survival of the animals over time (Fig. 5**H**).

Galangin-ciprofloxacin combinatorial therapy is effective against biofilm infection in a fish tail wound infection model

To further validate the combinatorial treatment of Galangin with ciprofloxacin to biofilm infection in vertebrate animal model, we then applied 25 μM Galangin-0.08 μg/ml ciprofloxacin combinatorial treatment against the Medaka fish wounds infection as described in the workflow (Fig. 6**A**). Medaka fish has transparent larvae fish bodies for description of infection establishment process via *in vivo* imaging techniques, and many research tools for studying gene functions can be utilized on Medaka [85,86]. The established Medaka-*P. aeruginosa* infection model on fish skin-wound provided a convenient, visible and cheap way to further validate antibacterial drugs [87].

We observed that bacterial populations in the biofilm was reduced (Fig. 6**B**). The Galangin-ciprofloxacin combinatorial treatment could effectively downregulate the GFP expression level of p$_{pvdA}$-*gfp* (Fig. 6**C**) and significantly lowered pyoverdine levels of wounds infection (Fig. 6**D**) from fluorescent images of treated

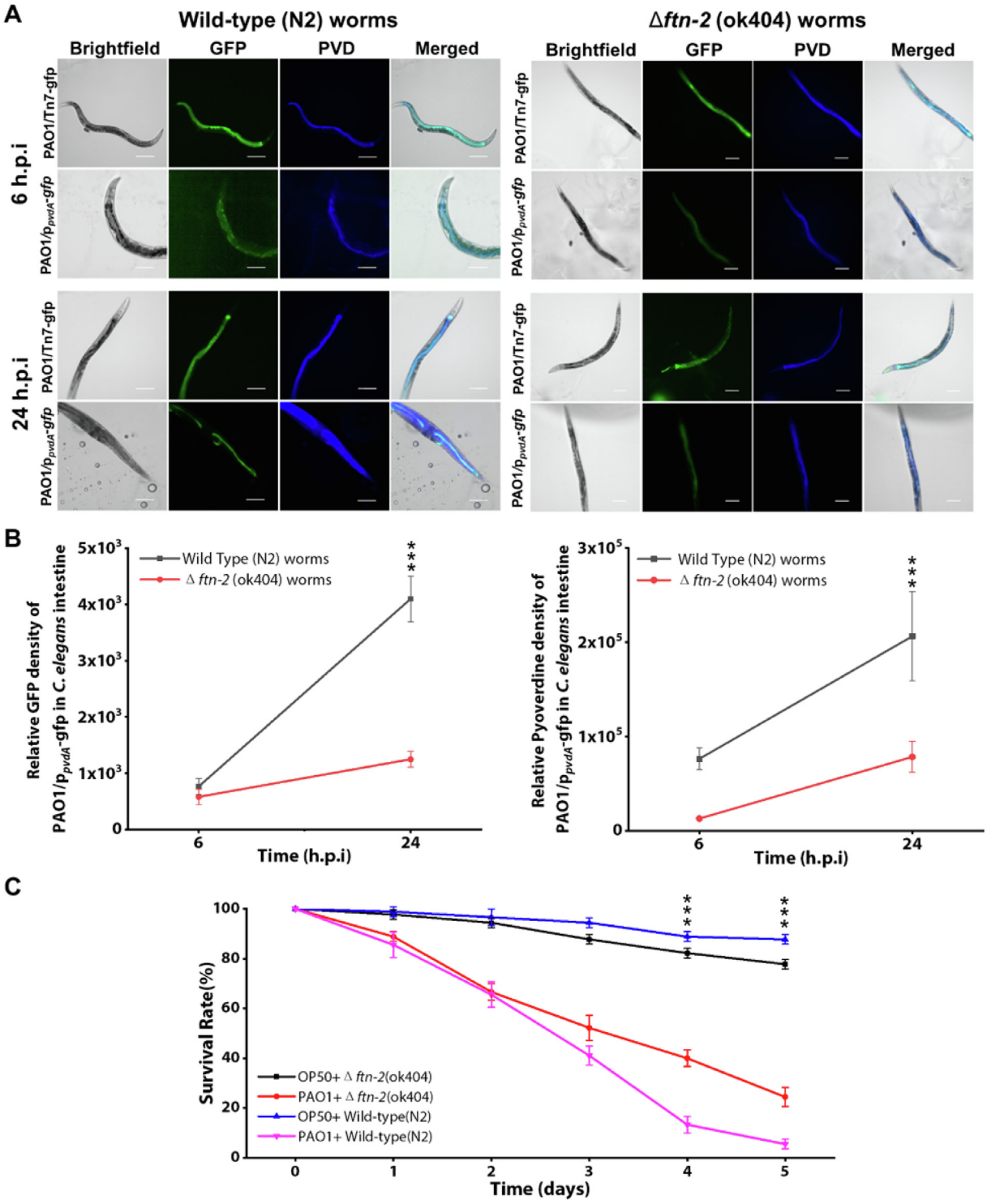

Fig. 4. Role of *FTN-2* by *Caenohabditis elegans* in iron competition during the bacterial infection interaction compared to wild type nematodes. (**A**) Representative fluorescent images of the fixed wild type (N2) and *ftn-2* (ok404) nematodes intestine after the infection of PAO1/Tn7-gfp and PAO1/p_{pvdA}-*gfp* from two time points (6 h.p.i and 24 h.p.i). (**B**) Relative GFP density and Pyoverdine density of the nematodes intestinal PAO1/p_{pvdA}-*gfp* biosensor between wild type nematodes and *ftn-2* (ok404) mutant nematodes over time. Both GFP promoted by PvdA and pyoverdine of *P. aeruginosa* had high expression in wild-type *C. elegans* intestine than *ftn-2* (ok404) *C. elegans*. (**C**) The survivability of wild-type *C. elegans* compared to *ftn-2* (ok404) *C. elegans* infected by PAO1 for 5 days. Compared to the wild type nematodes, *ftn-2* (ok404) nematodes had less competition with bacteria. H.p.i = hours post-infection. Scale bar: 100 μm. ***P < 0.001.

fishes wound (Fig. 6**E**). Hence, the Galangin-ciprofloxacin combinatorial treatment is safe and effective in eliminating the wound infection in the fish. Hence, we demonstrated that Galangin could be used as an inhibitor of bacterial pyoverdine to intercept host-pathogen iron competition and tilt the survival advantage to the host.

Discussion

Host-microbe interactions are important to the survival and growth of each species, so it is important to study how this relationship is important in human diseases and ecology by using biochemical approaches which can study proteomic expressions from

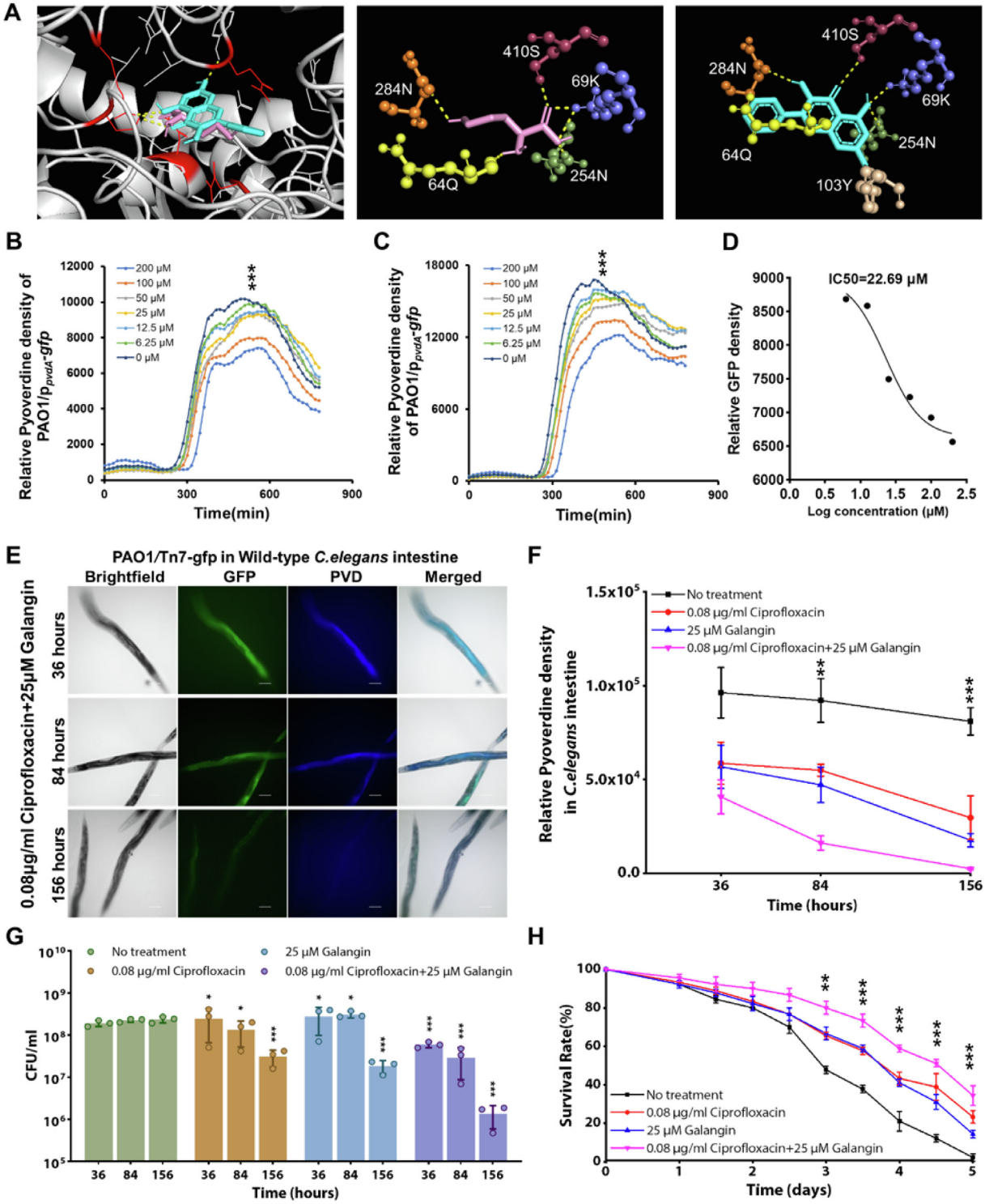

Fig. 5. Galangin serves as PvdA inhibitor that abrogates *Pseudomonas aeruginosa* intestinal infection. (**A**) Molecular docking revealed Galangin (blue) and ONH (pink) binding to amino acid residues in active sites of PvdA. (**B**) Galangin inhibits *in vitro pvdA* gene expression by testing GFP level of PAO1/p_{pvdA}-*gfp*. (**C**) Galangin inhibits *in vitro* pyoverdine production by testing fluorescent density. (**D**) The half-maximal inhibitory concentration (IC_{50}) graph of Galangin to *pvdA* expression and pyoverdine production inhibition. (**E**) Representative fluorescent images of fixed *C. elegans* intestine with Galangin and Ciprofloxacin treatment. (**F**) Relative pyoverdine density from wild type nematodes infected by PAO1 and then with the combinatorial treatment of Galangin and Ciprofloxacin. This combinatorial treatment can help to eliminate the intestinal *P. aeruginosa* infection in *C. elegans* in 156 h with several times of drug administration. (**G**) *P. aeruginosa* CFU in nematodes intestine after Galangin and/or Ciprofloxacin treatment for 5 days. Bacteria numbers show an alleviation of biofilm infection after combinatorial treatment. (**H**) Survival rate of wild type *C. elegans* with Galangin and Ciprofloxacin treatment. This combinatorial treatment could increase survival rate of host. Scale bar: 100 μm. ***P < 0.001, **P < 0.01, *P < 0.05.

both bacteria and host simultaneously. Our forward-reverse SILAC approach represents a technical advance in proteomics which solve the existing problem of studying either the host or microbe proteome in the same sample. Although there are computational improvements where dual species can be possibly searched and identified in a single mass spectrometry run [88,89], the strength

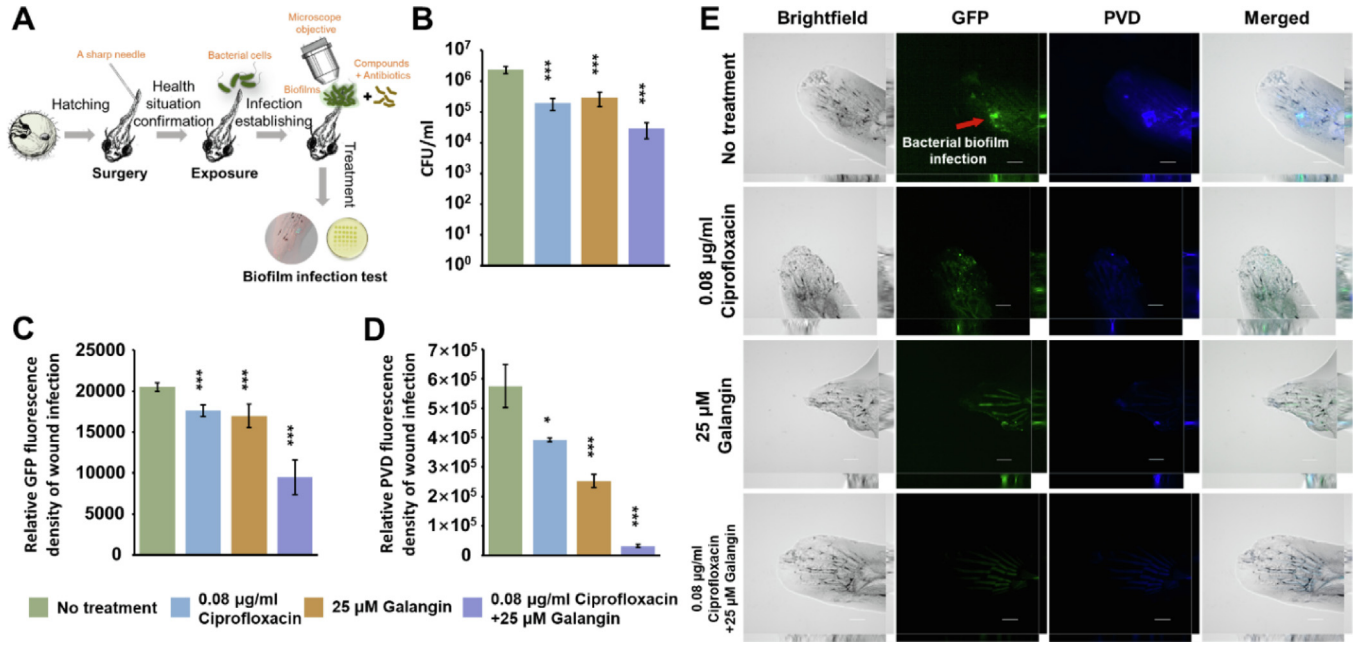

Fig. 6. Combinatorial treatment of ciprofloxacin and Galangin eliminates the wound infection caused by *Pseudomonas aeruginosa* on medaka fish tail. (**A**) The establishment of medaka fish – *P. aeruginosa* infection model for testing novel antimicrobial strategies *in vivo*. (**B**) The bacterial populations in the wound infection after treatment by monotherapy and combinatorial therapy of Galangin and ciprofloxacin. (**C**) Relative GFP fluorescence expression level of PAO1/p_{pvdA}-*gfp* on the wound infection after treatment by monotherapy and combinatorial therapy of Galangin and ciprofloxacin. (**D**) Pyoverdine expression level of in wound biofilm infection after monotherapy and combinatorial therapy of Galangin and ciprofloxacin. (**E**) Representative fluorescent images of wound bacterial (PAO1/p_{pvdA}-*gfp*) biofilms infection on medaka fish after treatment. GFP: green, and pyoverdine: blue. Scale bar: 100 μm. The mean and ± sd. from three experiments are shown. ***P < 0.001, **P < 0.01, *P < 0.05.

of our SILAC approach lies in its specificity and sensitivity, where any newly-synthesized proteins must arise from direct interaction between host and pathogen – something that computational improvements cannot achieve. Moreover, computational bias still exists in current models, where further normalization of samples using computational software is required. For instance, recent papers working on dual-species bacterial model will require normalization and checking for cross-identification between proteins from both species [90,91], but our method bypasses any potential computational bias.

Iron competition between host and pathogen has been studied extensively, but these studies evaluated only from the point of the host or pathogen [42–44,52]. Our proteomics data revealed the simultaneous upregulation of iron scavenging proteins from host and pathogen in the same animal infection model. We showed that intestinal *P. aeruginosa* downregulated AlgR, which led to increased expression of PvdA. This corroborated with a previous study that showed that deletion of AlgR resulted in increased pyoverdine production [92]. Correspondingly, we showed that *C. elegans* upregulated ferritin protein that participated in iron competition with pyoverdine. While a previous study had preliminarily shown that ferritin was expressed in *C. elegans* during the Gram positive *S. aureus* infection [49], we showed that pyoverdine from the Gram-negative *P. aeruginosa* was also the direct iron competitor of ferritin.

Interestingly, the ferritin-deficient *C. elegans* did not induce *P. aeruginosa*'s expression of pyoverdine, indicating that the ferritin-deficient host could not participate in iron competition and it 'takes two hands to clap' in host-pathogen interactions. This is surprising, because other studies had shown hosts which cannot compete for iron effectively with the pathogen possess lower immunity and face more severe infections [93]. This raises the need to pursue further studies on both positive and negative effects of inhibiting the host's iron response as a means to fight pathogenic infections. Nonetheless, other virulence mechanisms could also come into play during the infection process, where HCN and biofilm matrix could reduce *C. elegans* survival [46,55,94].

Lastly, intercepting host-pathogen iron competition by inhibiting iron siderophores or their synthesis pathways will tilt the favor against pathogen survival, thereby enabling better survival of the animal host. Moreover, *P. aeruginosa* clinical isolates often expressed high levels of pyoverdine gene expression, indicating the strong selection pressure driving pyoverdine synthesis and function during infections [95]. Hence, it is crucial to develop pyoverdine inhibitors that hinder *P. aeruginosa*'s ability to compete for iron from the host. While pyoverdine inhibitors had been developed to inhibit *P. aeruginosa* biofilms, they were mostly direct iron competitors which are not specific ones against pyoverdine synthesis enzymes [96]. We had identified and evaluated Galangin as a novel inhibitor of pyoverdine synthesis by PvdA. Galangin was previously shown to kill cancer cells and *Staphylococcus aureus* [97,98], but its MIC (22.69 μM) used in this study was significantly lower than the bactericidal concentration in millimolar range used in other studies [99]. To further improve Galangin effectiveness of a PvdA inhibitor, structure–activity relationship (SAR) studies may be conducted to modify Galangin's chemical structure in the future [100].

We also showed that Galangin could be used in combinatorial therapy with ciprofloxacin to effectively eradicate *P. aeruginosa* intestinal and skin infection. As the use of ciprofloxacin may lead to side-effects, such as nausea and diarrhea [101], it is important to study any possible complications attributed to the combinatorial Galangin-ciprofloxacin therapy. Alternatively, other antibiotics effective against *P. aeruginosa*, such as colistin [102], can be used in combination with Galangin to improve antimicrobial therapy against *P. aeruginosa* infections. In summary, advances in 'omics' approaches enable concurrent study of host and pathogen interactions, where the bacterial targets can be used to develop novel antimicrobial strategies against difficult-to-treat infections.

Conclusion

In conclusion, our proof-of-concept study developed the first SILAC proteomics approach which can simultaneously provide proteomic information of both host and pathogen in the same sample, with future applications in higher host organisms and other pathogenic microbes. This provides direct information about true host-pathogen interactions in the form of iron competition, where *C. elegans* upregulated its iron-competing ferritin in response to pyoverdine secreted by *P. aeruginosa*. Novel insights into intercepting the pathogen's iron-scavenging abilities will drive future development of anti-virulence strategies that intervene host-pathogen interactions.

Materials and methods

Growth and maintenance of bacterial strains and Caenorhabditis elegans

The bacterial strains and *C. elegans* used in this project were described in Supplementary Table 1. Medium for bacterial cultivation was Luria-Bertani (LB) broth (Difco, BD Company, USA), while Pseudomonas aeruginosa strains were grown in ABTGC (ABT minimal medium supplemented with 2 g/L glucose and 2 g/L casamino acids at 37 °C [103]. For plasmid maintenance in E. coli (Supplementary Table 1), the medium was supplemented with 100 μg ml^{-1} ampicillin and 15 μg ml^{-1} gentamicin. For marker selection in P. aeruginosa, 30 μg ml^{-1} gentamicin and 100 μg ml^{-1} streptomycin were used.

Nematode growth medium (NGM) agar and liquid worm assay medium [35] were used for *C. elegans* maintenance and experiments [104]. *C. elegans* used in this project were collected from the Caenorhabditis Genetics Center (CGC), the University of Minnesota. For animal cultivation, *Escherichia coli* OP50 bacterial lawn were cultivated on NGM agar plates at 37 °C for 16 h. The *C. elegans* was transferred to the NGM agar plates with OP50 lawn and cultivated at room temperature for 72 h to allow the population expansion. For the *C. elegans ftn-2*(ok404) mutant, the NGM agar containing 5 mg ml^{-1} ammonium ferric citrate was used as cultivation medium. Since standard infection assays typically use a range of 15 – 40 nematodes per plate for experiments [105–108], at least 30 nematodes per replicate plate, unless otherwise stated were used for our study.

SILAC proteomics assay

The *P. aeruginosa* lysine auxotrophic strain Δ*lysA* [50] was grown in the liquid ABTG medium with Amino acid Drop-out Mix Minus Lysine without Yeast Nitrogen Base powder (United States Biological, MA) and 500 μM ^{13}C- $_L$-lysine ($_L$-lysine:2HCl, U-13C6, 98 %, CIL, Inc, USA) labeled overnight. The overnight culture was filtered through the 0.22 μm filter (GTTP04700, Merck Millipore, America) by the vacuum suction filtration pump to collect the bacterial cells on the filters. The filters were placed on the ABTG agar with Amino acid Drop-out Mix Minus Lysine without Yeast Nitrogen Base powder and 500 μM ^{13}C- $_L$-lysine to enable biofilm lawn growth for 48 h at 37 °C [50]. The filter containing the biofilm lawn were next transferred to new NGM-ml agar, NGM agar minus lysine adding Amino acid Drop-out Mix Minus Lysine without Yeast Nitrogen Base powder and ^{12}C- $_L$-lysine additive ($_L$-lysine powder, ≥98 %, Sigma-Aldrich, USA), where around 100 L3 *C. elegans* animals pre-labelled with ^{12}C- $_L$-lysine were transferred from feeding plates to biofilm on filters. After 6 h.p.i and 24 h.p.i at 25 °C, all live nematodes were collected into 1.5 ml microcentrifuge tubes and washed by ice-cold PBS buffer via centrifugation for 10 times to remove bacteria retaining on the animal surface. Dead nematodes were not collected for proteomics. For the nematode samples, they were grinded to tissue fragments first before adding the ice-cold lysis buffer. The lysate was then sonicated and centrifuged to remove cellular debris pellet. Lysate protein concentration was determined by Pierce BCA Assay (Thermo Fisher Scientific, Franklin, Massachusetts) as per the manufacturer's instructions. Total protein was reduced with 10 mM 1,4-dithiothreitol (DTT) at 37 °C for 1 h and subsequently alkylated in 20 mM iodoacetamide (IAA) for 30 min at room temperature in the dark. Proteins were digested with Lys-C (1:100, w/w) at 37 °C for 2 h and then trypsin (1:100, w/w) at 37 °C overnight. All the tryptic peptides samples were desalted on a Sep-pak C18 cartridges column and then lyophilized under vacuum.

The vacuum-dried samples were resuspended in 0.1 % FA for liquid chromatography (LC)-MS/ MS analysis. Each sample of peptides was loaded onto a C18 trap column (75 μm ID×2 cm, 3 μm, Thermo Scientific) and then separated on a C18 analytical column (75 μm ID×50 cm, 2 μm, Thermo Scientific). Peptides were separated and analyzed on an Easy-nLC 1200 system coupled to a Q-Exactive HF-X Hybrid Quadrupole-Orbirap Mass spectrometer system (Thermo Fisher Scientific). Mobile phase A (0.1 % formic acid in 2 % ACN) and mobile phase B (0.1 % formic acid in 98 % ACN) were used to establish a 60 min gradient composed of 1 min of 6 % B, 48 min of 6–28 % B, 1 min of 28–60 %B, 1 min 60–90 % B, 9 min of 90 % B at a constant flow rate of 250 nl/min at 55℃. MS data were acquired using the following parameters: for all experiments, the instrument was operated in the data dependent mode. Peptides were then ionized by electrospray at 2.2 kV. Full scan MS spectra (from *m*/*z* 375 to 1500) were acquired in the Orbitrap at a high resolution of 60,000 with an automatic gain control (AGC) of 3×10^6 and a maximum fill time of 20 ms. The twenty most intense ions were sequentially isolated and fragmented in the HCD collision cell with normalized collision energy of 27 %. Fragmentation spectra were acquired in the Orbitrap analyzer with a resolution of 15,000. Ions selected for MS/MS were dynamically excluded for a duration of 30 s.

The raw data were processed and searched using Proteome Discoverer software (PD) (version 2.2.0.388). A *C. elegans* protein database (4306 entries, updated on 11–2019), a *P. aeruginosa* protein database (55,063 sequences, 17,906,244 residues, updated on 11-2019) and the database for proteomics contaminants from MaxQuant (298 entries) were used for database searches. Semi-trypsin was set as the enzyme, and two missed cleavage sites of trypsin were allowed. Mass error was set to 10 ppm for precursor ions and 0.02 Da for fragmented ions. Carbamidomethylation on Cys was specified as the fixed modification, and oxidation (M), acetylation (Protein N-term) and isotope labeling of lysine (+6.020 Da) were set as variable modifications. Reversed database searches were used to evaluate false discovery rate (FDR) of peptide and protein identifications. False discovery rate (FDR) thresholds for protein, peptide and modification site were specified at 1 %. Minimum peptide length was set at 7. All other parameters were set to default values. We used ANOVA (Background Based) tests to formalize p-value calculation and perform a multiple hypothesis testing correction on significantly different proteins, where the adjusted p-value was processed via Bonferroni-Holm method. Then the fold-change values and regulation situations of proteins of samples from 6 h.p.i to 24 h.p.i in bacterial and host groups were calculated and performed basing on the formulas respectively:

$$\text{For bacteria proteins}: \frac{\text{Abundance Ratio}: (6\text{h.p.i}, \text{Heavy})/(6\text{h.p.i}, \text{Light})}{\text{Abundance Ratio}: (24\text{h.p.i}, \text{Heavy})/(24\text{h.p.i}, \text{Light})}$$

For host animal proteins :

$$\frac{\text{Abundance Ratio : (24h.p.i} - 1, \text{Heavy)/(24h.p.i} - 1, \text{Light)}}{\text{Abundance Ratio : (6h.p.i} - 1, \text{Heavy)/(6h.p.i, Light)}}$$

The ratio was set with the 2-fold changes and p-value < 0.05. All the statistical calculation and data process were processed via MetaboAnalyst 5.0 and analysis in Language R. Liquid chromatography-mass spectrometry/mass spectrometry (LC–MS/MS) raw data of all replicates, results for protein and peptide identification and quantification from MaxQuant has been submitted to the ProteomeXchange Consortium as an integrated proteome resource [108].

Quantification of bacterial numbers in C. elegans intestine by colony forming unit (CFU)

After cultivation on the NGM plates with bacteria lawn, nematodes were washed 3 times with sterile 0.9 % (w/v) NaCl saline by centrifuging at 1000–2000 rpm for 30 sec. The nematodes were resuspended in 100 μl sterilized 0.9 % NaCl saline in 1.5 ml-microcentrifuge tubes (JET BIOFIL, China), followed by homogenization with pellet pestles. The homogenates were serially diluted in 0.9 % NaCl in 95-well plate (SPL Life Sciences company, South Korea) and subsequently cultivated on LB agar petri dishes at 37 °C for 16 h. After enumeration of colonies grown on agar plate, the CFU ml^{-1} were calculated by the following formula: colony number × dilution factor/volume. Experiments were performed in triplicates, and the results are shown as mean ± sd.

Structure-based virtual screening for potential PvdA inhibitors

As previously described [53,54], the software AutoDock Vina was employed to conduct molecule docking of PvdA protein active site to the chemical library *in silico*. Discovery studio 2016 Client was used to edit the PvdA protein by eliminating water molecules and adding polar hydrogens. All ligands' libraries were obtained from ZINC database. The OpenBabel GUI was used to convert the libraries into single ligand molecules. As reference ligand, N∼5 ∼ −hydroxy-L-ornithine (ONH for short) was used to detect primary bonding sites on PvdA protein. Each output result included 10 models which were evaluated and ranked by binding affinity energy. The 3D images of binding models were generated by PyMOL v.2.3.2, and PyMOL was also used to select the numbers of bonds to protein active site.

Inhibition and half maximal inhibitory concentrations (IC_{50}) testing

To evaluate the inhibitory effect of compounds on PvdA expression, the PAO1/p_{pvdA}-*gfp* [109] was cultivated in ABTGC medium containing a range of Galangin concentrations (0–200 μM) in triplicate wells of a 96-well plate (SPL Life Sciences company, South Korea). The 96-well plate was incubated at 37 °C for 16 h in a microplate reader (Tecan Infinite M1000 Pro, Switzerland) for analysis of optical density at 600 nm (OD600). GFP (Ex: 495 nm, Em: 515 nm) and pyoverdine (Ex: 400 nm, Em: 450 nm) every 15 mins. The half-maximal inhibitory concentration (IC_{50}) was calculated by GraphPad Prism 8.0.2 software (GraphPad Software Inc., USA). Experiments were performed in triplicate, and the results were shown as the mean ± sd.

C. elegans killing assay

P. aeruginosa strains were cultivated on NGM agar plates at 37 °C for 16 h, followed by transfer of 30 individuals of L3 *C. elegans* from OP50 feeding plate to *P. aeruginosa* lawn by titanium wire picker [52]. Live and dead animals were enumerated daily to evaluate the killing assay of *C. elegans*.

Galangin-ciprofloxacin combinatorial treatment against C. elegans intestinal infection

The infected *C. elegans* were treated with monotherapy or combinatorial therapy of Galangin and ciprofloxacin in a liquid worm assay medium [35] for 7–8 h daily for 156 h (6 days). After drug treatment, the live and dead *C. elegans* were enumerated. Experiments were performed in triplicates, and the results are shown as mean ± sd.

Epifluorescence microscopy

For epifluorescence microscopy of intestinal bacteria in the nematodes [34], the live nematodes were first collected and then fixed in μ-Slide 8-well plates (Ibidi, Germany) containing 2 % agarose + 4 % paraformaldehyde (Sigma Aldrich, USA). All microscopy images with Z-stack were captured and acquired by using Nikon Eclipse Ti2-E Live-cell Fluorescence Imaging System with 20 × objective using Brightfield, GFP (Ex: 495 nm, Em: 515 nm) and pyoverdine (Ex: 400 nm, Em: 450 nm) fluorescent channels. As autofluorescence of the entire nematode body across a wide range of fluorescent spectrum poses a problem for microscopy [110], it is important to ensure that only bacterial fluorescence within the intestine were observed and measured. At least 5 images were captured for every sample. All the images were exported by the NIS (Nikon) program with 100 μm scale bars in all images.

Tabulation of relative fluorescence density

As previously described [53], relative fluorescence levels in the images were quantified by ImageJ program using the equation: corrected total cell fluorescence (CTCF) = Integrated Density – (Area of selected cell × Mean fluorescence of background readings). Experiments were performed in triplicate, and results were shown as the mean ± sd.

Ethics statement

All experiments involving Medaka fish were conducted according to the ethical policies and procedures approved by the ethics committee of the City University of Hong Kong animal research ethics committee, with permit number Ref. No. A-0418. All Medaka fish experiments were performed according to the guidance of the Department of Health in Hong Kong.

Galangin-ciprofloxacin combinatorial treatment against Medaka wounds infection

The Medaka fish cultivation and the wounds infection on fishes were processed and established as previously described [87]. The infected fishes were treated with monotherapy or combinatorial therapy of Galangin and ciprofloxacin in sterile culture water for 6 h. These treated fishes were anesthetized by immersing the animals in 0.015 μM anesthesia tricaine mesylate (MS 222) (Merck KGaA, USA) for CFU test and fluorescence images capturing. Experiments were performed in triplicates, and the results are shown as mean ± sd.

Statistical analysis

The results were expressed as means ± standard deviation. Using GraphPad Prism, all data sets were evaluated using the

one-way ANOVA and Student's *t*-test to study the associations between independent variables and calculate the *p*-values. For post-hoc tests, the Fisher's least significant difference (LSD) Test, Tukey's Test and Duncan's new multiple range test was used.

Data and materials availability

All data are available in the main text or the supplementary materials. The mass spectrometry proteomics raw data have been deposited to the ProteomeXchange Consortium (https://proteomecentral.proteomexchange.org) via the iProX partner repository with the dataset identifier PXD036121.

Credit author statement

S.L.C designed methods and experiments. Y.S.L and C.Z performed laboratory experiments, analysed the data, and interpreted the results. P.H analysed the data. S.L.C and Y.S.L, wrote the paper. All authors have contributed to, seen, and approved the manuscript.

Compliance with ethics requirements

All Institutional and National Guidelines for the care and use of animals (fisheries) were followed.

Declaration of competing interest

The authors declare that they have no known competing financial interests or personal relationships that could have appeared to influence the work reported in this paper.

Acknowledgments

This research is supported by The Hong Kong Polytechnic University, Department of Applied Biology and Chemical Technology Startup Grant (BE2B), State Key Laboratory of Chemical Biology and Drug Discovery Fund (1-BBX8), Departmental General Research Fund (UALB), One-line account (ZVVV), Environmental and Conservation Fund (ECF-48/2019), Health and Medical Research Fund (HMRF-201903032), Gifted Education Fund (2020-06) and Pneumoconiosis Compensation Fund Board (ZJN2).

We sincerely thank Prof Haihua Liang, Northwest University, for the generous gift of the ΔalgR mutant. The C. elegans strains were provided by the CGC, which is funded by NIH Office of Research Infrastructure Programs (P40 OD010440).

Appendix A. Supplementary material

Supplementary data to this article can be found online at https://doi.org/10.1016/j.jare.2024.08.038.

References

[1] Bottek J, Soun C, Lill JK, Dixit A, Thiebes S, Beerlage A-L, et al. Spatial proteomics revealed a CX3CL1-dependent crosstalk between the urothelium and relocated macrophages through IL-6 during an acute bacterial infection in the urinary bladder. Mucosal Immunol 2020;13(4):702–14.
[2] Kamaladevi A, Marudhupandiyan S, Balamurugan K. Model system based proteomics to understand the host response during bacterial infections. Mol Biosyst 2017;13(12):2489–97.
[3] Shui W, Gilmore SA, Sheu L, Liu J, Keasling JD, Bertozzi CR. Quantitative proteomic profiling of host-pathogen interactions: the macrophage response to *Mycobacterium tuberculosis* lipids. J Proteome Res 2009;8(1):282–9.
[4] Munday DC, Surtees R, Emmott E, Dove BK, Digard P, Barr JN, et al. Using SILAC and quantitative proteomics to investigate the interactions between viral and host proteomes. Proteomics 2012;12(4–5):666–72.
[5] Shi L, Adkins JN, Coleman JR, Schepmoes AA, Dohnkova A, Mottaz HM, et al. Proteomic analysis of *Salmonella enterica* serovar typhimurium isolated from RAW 264.7 macrophages: identification of a novel protein that contributes to the replication of serovar typhimurium inside macrophages. J Biol Chem 2006;281(39):29131–40.
[6] Sukumaran A, Woroszchuk E, Ross T, Geddes-McAlister J. Proteomics of host-bacterial interactions: new insights from dual perspectives. Can J Microbiol 2021;67(3):213–25.
[7] Edwards RJ, Pyzio M, Gierula M, Turner CE, Abdul-Salam VB, Sriskandan S. Proteomic analysis at the sites of clinical infection with invasive *Streptococcus pyogenes*. Sci Rep 2018;8(1):5950.
[8] Yu X, Decker KB, Barker K, Neunuebel MR, Saul J, Graves M, et al. Host-pathogen interaction profiling using self-assembling human protein arrays. J Proteome Res 2015;14(4):1920–36.
[9] Ong SE, Blagoev B, Kratchmarova I, Kristensen DB, Steen H, Pandey A, et al. Stable isotope labeling by amino acids in cell culture, SILAC, as a simple and accurate approach to expression proteomics. Mol Cell Proteom: MCP 2002;1(5):376–86.
[10] Lau H-T, Suh HW, Golkowski M, Ong S-E. Comparing SILAC- and stable isotope dimethyl-labeling approaches for quantitative proteomics. J Proteome Res 2014;13(9):4164–74.
[11] Wang X, He Y, Ye Y, Zhao X, Deng S, He G, et al. SILAC–based quantitative MS approach for real-time recording protein-mediated cell-cell interactions. Sci Rep 2018;8(1):8441.
[12] Georgianna DR, Hawkridge AM, Muddiman DC, Payne GA. Temperature-dependent regulation of proteins in *Aspergillus flavus*: whole organism stable isotope labeling by amino acids. J Proteome Res 2008;7(7):2973–9.
[13] Beati H, Langlands A, Ten Have S, Müller HJ. SILAC-based quantitative proteomic analysis of *Drosophila* gastrula stage embryos mutant for fibroblast growth factor signalling. Fly (Austin) 2020;14(1–4):10–28.
[14] Bjarnsholt T. The role of bacterial biofilms in chronic infections. APMIS 2013;121(s136):1–58.
[15] Romling U, Balsalobre C. Biofilm infections, their resilience to therapy and innovative treatment strategies. J Intern Med 2012;272(6):541–61.
[16] Costerton JW, Stewart PS, Greenberg EP. Bacterial biofilms: a common cause of persistent infections. Science 1999;284(5418):1318.
[17] Høiby N, Bjarnsholt T, Givskov M, Molin S, Ciofu O. Antibiotic resistance of bacterial biofilms. Int J Antimicrob Agents 2010;35(4):322–32.
[18] Domenech M, Ramos-Sevillano E, García E, Moscoso M, Yuste J. Biofilm formation avoids complement immunity and phagocytosis of *Streptococcus pneumoniae*. Infect Immun 2013;81(7):2606–15.
[19] Boucher HW, Scheld M, Bartlett J, Talbot GH, Bradley JS, Spellberg B, et al. Bad bugs, no drugs: No ESKAPE! An update from the infectious diseases Society of America. Clin Infect Dis 2009;48(1):1–12.
[20] Kang CI, Kim SH, Kim HB, Park SW, Choe YJ, Oh MD, et al. *Pseudomonas aeruginosa* bacteremia: risk factors for mortality and influence of delayed receipt of effective antimicrobial therapy on clinical outcome. Clin Infect Dis 2003;37(6):745–51.
[21] Vitkauskiene A, Skrodeniene E, Dambrauskiene A, Macas A, Sakalauskas R. Pseudomonas aeruginosa bacteremia: resistance to antibiotics, risk factors, and patient mortality. Medicina (Kaunas) 2010;46(7):490–5.
[22] Smith EE, Buckley DG, Wu Z, Saenphimmachak C, Hoffman LR, D'Argenio DA, et al. Genetic adaptation by *Pseudomonas aeruginosa* to the airways of cystic fibrosis patients. Proc Natl Acad Sci 2006;103(22):8487–92.
[23] Chuang C-H, Wang Y-H, Chang H-J, Chen H-L, Huang Y-C, Lin T-Y, et al. Shanghai fever: a distinct *Pseudomonas aeruginosa* enteric disease. Gut 2014;63(5):736–43.
[24] Moran H, Yaniv I, Ashkenazi S, Schwartz M, Fisher S, Levy I. Risk factors for typhlitis in pediatric patients with cancer. J Pediatr Hematol Oncol 2009;31(9):630–4.
[25] Mullassery D, Bader A, Battersby AJ, Mohammad Z, Jones ELL, Parmar C, et al. Diagnosis, incidence, and outcomes of suspected typhlitis in oncology patients—experience in a tertiary pediatric surgical center in the United Kingdom. J Pediatr Surg 2009;44(2):381–5.
[26] Rowe MI, Reblock KK, Kurkchubasche AG, Healey PJ. Necrotizing enterocolitis in the extremely low birth weight infant. J Pediatr Surg 1994;29(8):987–91.
[27] Zaborina O, Kohler JE, Wang Y, Bethel C, Shevchenko O, Wu L, et al. Identification of multi-drug resistant *Pseudomonas aeruginosa* clinical isolates that are highly disruptive to the intestinal epithelial barrier. Ann Clin Microbiol Antimicrob 2006;5(1):14.
[28] Spernovasilis N, Psichogiou M, Poulakou G. Skin manifestations of *Pseudomonas aeruginosa* infections. Curr Opin Infect Dis 2021;34(2).
[29] Wu DC, Chan WW, Metelitsa AI, Fiorillo L, Lin AN. *Pseudomonas* Skin Infection. Am J Clin Dermatol 2011;12(3):157–69.
[30] Thi MTT, Wibowo D, Rehm BHA. Pseudomonas aeruginosa Biofilms. Int J Mol Sci 2020;21(22).
[31] Banin E, Vasil ML, Greenberg EP. Iron and *Pseudomonas aeruginosa*> biofilm formation. Proc Nat Acad Sci. 2005;102(31):11076-81.
[32] Chen Y, Yuan M, Mohanty A, Yam JKH, Liu Y, Chua SL, et al. Multiple diguanylate cyclase-coordinated regulation of pyoverdine synthesis in *Pseudomonas aeruginosa*. Environ Microbiol Rep 2015;7(3):498–507.

[33] Valentini M, Filloux A. Biofilms and Cyclic di-GMP (c-di-GMP) Signaling: Lessons from *Pseudomonas aeruginosa* and Other Bacteria. J Biol Chem 2016;291(24):12547–55.
[34] Chan SY, Liu SY, Wu R, Wei W, Fang J-K-H, Chua SL. Simultaneous dissemination of nanoplastics and antibiotic resistance by nematode couriers. Environ Sci Tech 2023;57(23):8719–27.
[35] Chua SL, Liu Y, Yam JK, Chen Y, Vejborg RM, Tan BG, et al. Dispersed cells represent a distinct stage in the transition from bacterial biofilm to planktonic lifestyles. Nat Commun 2014;5:4462.
[36] Fabian DK, Fuentealba M, Dönertaş HM, Partridge L, Thornton JM. Functional conservation in genes and pathways linking ageing and immunity. Immun Ageing 2021;18(1):23.
[37] Treitz C, Cassidy L, Höckendorf A, Leippe M, Tholey A. Quantitative proteome analysis of *Caenorhabditis elegans* upon exposure to nematicidal *Bacillus thuringiensis*. J Proteomics 2015;113:337–50.
[38] Bogaerts A, Beets I, Temmerman L, Schoofs L, Verleyen P. Proteome changes of *Caenorhabditis elegans* upon a *Staphylococcus aureus* infection. Biol Direct 2010;5:11.
[39] Bogaerts A, Temmerman L, Boerjan B, Husson SJ, Schoofs L, Verleyen P. A differential proteomics study of *Caenorhabditis elegans* infected with *Aeromonas hydrophila*. Dev Comp Immunol 2010;34(6):690–8.
[40] Durai S, Singh N, Kundu S, Balamurugan K. Proteomic investigation of *Vibrio alginolyticus* challenged *Caenorhabditis elegans* revealed regulation of cellular homeostasis proteins and their role in supporting innate immune system. Proteomics 2014;14(15):1820–32.
[41] Munguia J, Nizet V. Pharmacological targeting of the host-pathogen interaction: alternatives to classical antibiotics to combat drug-resistant superbugs. Trends Pharmacol Sci 2017;38(5):473–88.
[42] Flo TH, Smith KD, Sato S, Rodriguez DJ, Holmes MA, Strong RK, et al. Lipocalin 2 mediates an innate immune response to bacterial infection by sequestrating iron. Nature 2004;432(7019):917–21.
[43] Perry WJ, Spraggins JM, Sheldon JR, Grunenwald CM, Heinrichs DE, Cassat JE, et al. *Staphylococcus aureus* exhibits heterogeneous siderophore production within the vertebrate host. Proc Nat Acad Sci. 2019;116(44): 21980-2.
[44] Skaar EP. The battle for iron between bacterial pathogens and their vertebrate hosts. PLoS Pathog 2010;6(8).
[45] Hammer ND, Skaar EP. Molecular mechanisms of *Staphylococcus aureus* iron acquisition. Annu Rev Microbiol 2011;65:129–47.
[46] Chan SY, Liu SY, Seng Z, Chua SL. Biofilm matrix disrupts nematode motility and predatory behavior. ISME J 2021;15(1):260–9.
[47] Ma Y, Deng Y, Hua H, Khoo BL, Chua SL. Distinct bacterial population dynamics and disease dissemination after biofilm dispersal and disassembly. ISME J 2023.
[48] Ma Y, Aung TT, Lakshminarayanan R, Chua SL. Biofilm formation and virulence potential of carbapenem-resistant *Pseudomonas aeruginosa*. The Lancet Microbe 2023;4(7):e489.
[49] Simonsen KT, Møller-Jensen J, Kristensen AR, Andersen JS, Riddle DL, Kallipolitis BH. Quantitative proteomics identifies ferritin in the innate immune response of *C. elegans*. Virulence 2011;2(2):120–30.
[50] Chua SL, Yam JK, Hao P, Adav SS, Salido MM, Liu Y, et al. Selective labelling and eradication of antibiotic-tolerant bacterial populations in *Pseudomonas aeruginosa* biofilms. Nat Commun 2016;7:10750.
[51] Yeung YWS, Ma Y, Deng Y, Khoo BL, Chua SL. Bacterial Iron Siderophore Drives Tumor Survival and Ferroptosis Resistance in a Biofilm-Tumor Spheroid Coculture Model. Advanced Science.n/a(n/a):2404467.
[52] Hu M, Ma Y, Chua SL. Bacterivorous nematodes decipher microbial iron siderophores as prey cue in predator–prey interactions. Proceedings of the National Academy of Sciences. 2024;121(3):e2314077121.
[53] Ma Y, Tang WS, Liu SY, Khoo BL, Chua SL. Juglone as a Natural Quorum Sensing Inhibitor against *Pseudomonas aeruginosa* pqs-Mediated Virulence and Biofilms. ACS Pharmacol Transl Sci 2024;7(2):533–43.
[54] Mok N, Chan SY, Liu SY, Chua SL. Vanillin inhibits PqsR-mediated virulence in *Pseudomonas aeruginosa*. Food Funct 2020;11(7):6496–508.
[55] Li S, Liu SY, Chan SY, Chua SL. Biofilm matrix cloaks bacterial quorum sensing chemoattractants from predator detection. ISME J 2022.
[56] Kotowski U, Erović BM, Schnöll J, Stanek V, Janik S, Steurer M, et al. Quantitative proteome analysis of Merkel cell carcinoma cell lines using SILAC. Clin Proteomics 2019;16(1):42.
[57] Geiger T, Cox J, Ostasiewicz P, Wisniewski JR, Mann M. Super-SILAC mix for quantitative proteomics of human tumor tissue. Nat Methods 2010;7 (5):383–5.
[58] Phillips NJ, Steichen CT, Schilling B, Post DMB, Niles RK, Bair TB, et al. Proteomic Analysis of *Neisseria gonorrhoeae* Biofilms Shows Shift to Anaerobic Respiration and Changes in Nutrient Transport and Outermembrane Proteins. PLoS One 2012;7(6).
[59] Post DMB, Held JM, Ketterer MR, Phillips NJ, Sahu A, Apicella MA, et al. Comparative analyses of proteins from *Haemophilus influenzae* biofilm and planktonic populations using metabolic labeling and mass spectrometry. BMC Microbiol 2014;14(1):329.
[60] Zečić A, Dhondt I, Braeckman BP. The nutritional requirements of *Caenorhabditis elegans*. Genes Nutr 2019;14:15 -.
[61] Larance M, Bailly AP, Pourkarimi E, Hay RT, Buchanan G, Coulthurst S, et al. Stable-isotope labeling with amino acids in nematodes. Nat Methods 2011;8 (10):849–51.
[62] Harris TW, Arnaboldi V, Cain S, Chan J, Chen WJ, Cho J, et al. WormBase: a modern model organism information resource. Nucleic Acids Res 2020;48 (D1):D762–7.
[63] Winsor GL, Griffiths EJ, Lo R, Dhillon BK, Shay JA, Brinkman FS. Enhanced annotations and features for comparing thousands of *Pseudomonas* genomes in the Pseudomonas genome database. Nucleic Acids Res 2016;44(D1): D646–53.
[64] Cox J, Neuhauser N, Michalski A, Scheltema RA, Olsen JV, Mann M. Andromeda: a peptide search engine Integrated into the MaxQuant Environment. J Proteome Res 2011;10(4):1794–805.
[65] Pang Z, Zhou G, Ewald J, Chang L, Hacariz O, Basu N, et al. Using MetaboAnalyst 5.0 for LC–HRMS spectra processing, multi-omics integration and covariate adjustment of global metabolomics data. Nat Protoc 2022;17(8):1735–61.
[66] Wang C, Tang Y, Wang Y, Li G, Wang L, Li Y. Label-free quantitative proteomics identifies Smarca4 is involved in vascular calcification. Ren Fail 2019;41(1):220–8.
[67] Brinkman FSL, Hancock REW, Stover CK. Sequencing solution: use volunteer annotators organized via Internet. Nature 2000;406(6799):933.
[68] Moreau-Marquis S, Stanton BA, O'Toole GA. *Pseudomonas aeruginosa* biofilm formation in the cystic fibrosis airway. Pulm Pharmacol Ther 2008;21 (4):595–9.
[69] King CD, Singh D, Holden K, Govan AB, Keith SA, Ghazi A, et al. Proteomic identification of virulence-related factors in young and aging C. elegans infected with *Pseudomonas aeruginosa*. J Proteomics 2018;181:92–103.
[70] Deretic V, Dikshit R, Konyecsni WM, Chakrabarty AM, Misra TK. The algR gene, which regulates mucoidy in *Pseudomonas aeruginosa*, belongs to a class of environmentally responsive genes. 1989;171(3):1278-83.
[71] Meneely KM, Barr EW, Bollinger Jr JM, Lamb AL. Kinetic mechanism of ornithine hydroxylase (PvdA) from *Pseudomonas aeruginosa*: substrate triggering of O2 addition but not flavin reduction. Biochemistry 2009;48 (20):4371–6.
[72] Kong W, Zhao J, Kang H, Zhu M, Zhou T, Deng X, et al. ChIP-seq reveals the global regulator AlgR mediating cyclic di-GMP synthesis in *Pseudomonas aeruginosa*. Nucl Acids Res 2015;43(17):8268–82.
[73] Little AS, Okkotsu Y, Reinhart AA, Damron FH, Barbier M, Barrett B, et al. *Pseudomonas aeruginosa* AlgR Phosphorylation Status Differentially Regulates Pyocyanin and Pyoverdine Production. 2018;9(1):e02318-17.
[74] Visca P, Ciervo A, Orsi N. Cloning and nucleotide sequence of the pvdA gene encoding the pyoverdin biosynthetic enzyme L-ornithine N5-oxygenase in *Pseudomonas aeruginosa*. J Bacteriol 1994;176(4):1128–40.
[75] Gourley BL, Parker SB, Jones BJ, Zumbrennen KB, Leibold EA. Cytosolic Aconitase and Ferritin Are Regulated by Iron in *Caenorhabditis elegans* *. J Biol Chem 2003;278(5):3227–34.
[76] Kang D, Kirienko DR, Webster P, Fisher AL, Kirienko NV. Pyoverdine, a siderophore from *Pseudomonas aeruginos*a, translocates into C. elegans, removes iron, and activates a distinct host response. Virulence 2018;9 (1):804–17.
[77] Little AS, Okkotsu Y, Reinhart AA, Damron FH, Barbier M, Barrett B, et al. *Pseudomonas aeruginosa* AlgR phosphorylation status differentially regulates pyocyanin and pyoverdine production. MBio 2018;9(1):e02318–10417.
[78] Anderson CP, Leibold EA. Mechanisms of iron metabolism in *Caenorhabditis elegans*. 2014;5.
[79] Liu Y, Yang L, Molin S. Synergistic activities of an efflux pump inhibitor and iron chelators against *Pseudomonas aeruginosa* growth and biofilm formation. Antimicrob Agents Chemother 2010;54(9):3960–3.
[80] Qiu DH, Huang ZL, Zhou T, Shen C, Hider RC. In vitro inhibition of bacterial growth by iron chelators. FEMS Microbiol Lett 2011;314(2):107–11.
[81] Imperi F, Massai F, Facchini M, Frangipani E, Visaggio D, Leoni L, et al. Repurposing the antimycotic drug flucytosine for suppression of *Pseudomonas aeruginosa* pathogenicity. Proc Nat Acad Sci 2013;110(18):7458-63.
[82] Olucha J, Meneely KM, Chilton AS, Lamb AL. Two Structures of an N-Hydroxylating Flavoprotein Monooxygenase: ORNITHINE HYDROXYLASE FROM *PSEUDOMONAS AERUGINOSA*. J Biol Chem 2011;286(36):31789–98.
[83] Barry AL, Jones RN, Thornsberry C, Ayers LW, Gerlach EH, Sommers HM. Antibacterial activities of ciprofloxacin, norfloxacin, oxolinic acid, cinoxacin, and nalidixic acid. 1984;25(5):633-7.
[84] McCloskey MC, Shaheen S, Rabago L, Hulverson MA, Choi R, Barrett LK, et al. Evaluation of in vitro and in vivo antibiotic efficacy against a novel bioluminescent *Shigella flexneri*. Sci Rep 2019;9(1):13567.
[85] Wakamatsu Y, Pristyazhnyuk S, Kinoshita M, Tanaka M, Ozato K. The see-through medaka: A fish model that is transparent throughout life. Proc Nat Acad Sci. 2001;98(18):10046-50.
[86] Furusawa R, Okinaka Y, Nakai T. Betanodavirus infection in the freshwater model fish medaka (Oryzias latipes). 2006;87(8):2333-9.
[87] Liu YS, Deng Y, Chen CK, Khoo BL, Chua SL. Rapid detection of microorganisms in a fish infection microfluidics platform. J Hazard Mater 2022;431:128572.
[88] Bozan M, Schmidt M, Musat N, Schmid A, Adrian L, Bühler K. Spatial organization and proteome of a dual-species cyanobacterial biofilm alter among N2-fixing and non-fixing conditions. mSystems 2023;8(3): e00302–23.
[89] Rytter H, Roger K, Chhuon C, Ding X, Coureuil M, Jamet A, et al. Dual proteomics of infected macrophages reveal bacterial and host players involved in the *Francisella* intracellular life cycle and cell to cell dissemination by merocytophagy. Sci Rep 2024;14(1):7797.

[90] Ali Mohammed MM, Pettersen VK, Nerland AH, Wiker HG, Bakken V. Label-free quantitative proteomic analysis of the oral bacteria *Fusobacterium nucleatum* and *Porphyromonas gingivalis* to identify protein features relevant in biofilm formation. Anaerobe 2021;72(1):102449.
[91] Mohammed MMA, Pettersen VK, Nerland AH, Wiker HG, Bakken V. Quantitative proteomic analysis of extracellular matrix extracted from mono- and dual-species biofilms of *Fusobacterium nucleatum* and *Porphyromonas gingivalis*. Anaerobe 2017;44:133–42.
[92] Little AS, Okkotsu Y, Reinhart AA, Damron FH, Barbier M, Barrett B, et al. P*seudomonas aeruginosa* AlgR Phosphorylation Status Differentially Regulates Pyocyanin and Pyoverdine Production. MBio 2018;9(1).
[93] Abuga KM, Nairz M, MacLennan CA, Atkinson SH. Severe anaemia, iron deficiency, and susceptibility to invasive bacterial infections. Wellcome Open Res 2023;8:48.
[94] Gallagher LA, Manoil C. *Pseudomonas aeruginosa* PAO1 Kills *Caenorhabditis elegans* by Cyanide Poisoning. J Bacteriol 2001;183(21):6207–14.
[95] Kang D, Revtovich AV, Chen Q, Shah KN, Cannon CL, Kirienko NV. Pyoverdine-dependent virulence of *Pseudomonas aeruginosa* Isolates from cystic fibrosis patients. Front Microbiol 2019;10:2048.
[96] Kirienko DR, Kang D, Kirienko NV. Novel pyoverdine inhibitors mitigate *Pseudomonas aeruginosa* pathogenesis. Front Microbiol 2019;9(3317).
[97] Jin Y, Yang P, Wang L, Gao Z, Lv J, Cui Z, et al. Galangin as a direct inhibitor of vWbp protects mice from *Staphylococcus aureus*-induced pneumonia. J Cell Mol Med 2022;26(3):828–39.
[98] Lee C-C, Lin M-L, Meng M, Chen S-S. Galangin induces p53-independent S-phase arrest and apoptosis in human nasopharyngeal carcinoma cells through inhibiting PI3K–AKT signaling pathway. Anticancer Res 2018;38 (3):1377–89.
[99] Pepeljnjak S, Kosalec I. Galangin expresses bactericidal activity against multiple-resistant bacteria: MRSA, *Enterococcus* spp. and *Pseudomonas aeruginosa*. FEMS Microbiol Lett 2004;240(1):111–6.
[100] Kim H, Choi JM, Choi Y, Tahir MN, Yang Y-H, Cho E, et al. Enhanced solubility of galangin based on the complexation with methylated microbial cyclosophoraoses. J Incl Phenom Macrocycl Chem 2014;79(3):291–300.
[101] Molnar DM, Kremzner ME. Fluoroquinolones: a hot topic for pharmacists and the food and drug administration's division of drug information. J Am Pharm Assoc 2019;59(1):13–6.
[102] Jangra V, Sharma N, Chhillar AK. Therapeutic approaches for combating *Pseudomonas aeruginosa* infections. Microbes Infect 2022;24(4):104950.
[103] Chua SL, Tan SY, Rybtke MT, Chen Y, Rice SA, Kjelleberg S, et al. Bis-(3'-5')-cyclic dimeric GMP regulates antimicrobial peptide resistance in *Pseudomonas aeruginosa*. Antimicrob Agents Chemother 2013;57(5):2066–75.
[104] Lewis JA, Fleming JT. Chapter 1 Basic Culture Methods. In: Epstein HF, Shakes DC, editors. Methods Cell Biol. 48: Academic Press; 1995. p. 3-29.
[105] Zhu J, Cai X, Harris Tyler L, Gooyit M, Wood M, Lardy M, et al. Disarming *Pseudomonas aeruginosa* virulence Factor LASB by leveraging a caenorhabditis elegans infection model. Chem Biol 2015;22(4):483–91.
[106] Tan M-W, Rahme LG, Sternberg JA, Tompkins RG, Ausubel FM. *Pseudomonas aeruginosa* killing of *Caenorhabditis elegans* used to identify *P. aeruginosa* virulence factors. Proc Nat Acad Sci. 1999;96(5):2408-13.
[107] Bogaerts A, Beets I, Temmerman L, Schoofs L, Verleyen P. Proteome changes of *Caenorhabditis elegans* upon a *Staphylococcus aureus* infection. Biol Direct 2010;5:11.
[108] Ma J, Chen T, Wu S, Yang C, Bai M, Shu K, et al. iProX: an integrated proteome resource. Nucleic Acids Res 2019;47(D1):D1211–7.
[109] Tan SY, Liu Y, Chua SL, Vejborg RM, Jakobsen TH, Chew SC, et al. Comparative systems biology analysis to study the mode of action of the isothiocyanate compound Iberin on *Pseudomonas aeruginosa*. Antimicrob Agents Chemother 2014;58(11):6648–59.
[110] Pincus Z, Mazer TC, Slack FJ. Autofluorescence as a measure of senescence in *C. elegans*: look to red, not blue or green. Aging (Albany NY) 2016;8 (5):889–98.